EC Journals.ASM.org

Identification of Hypoxia-Inducible Target Genes of *Aspergillus fumigatus* by Transcriptome Analysis Reveals Cellular Respiration as an Important Contributor to Hypoxic Survival

Kristin Kroll,[a] Vera Pähtz,[a,g] Falk Hillmann,[a,e] Yakir Vaknin,[f] Wolfgang Schmidt-Heck,[b] Martin Roth,[c] Ilse D. Jacobsen,[d] Nir Osherov,[f] Axel A. Brakhage,[a,e] Olaf Kniemeyer[a,e,g]

Department of Molecular and Applied Microbiology,[a] Research Group Systems Biology/Bioinformatics,[b] Bio Pilot Plant,[c] and Research Group Microbial Immunology,[d] the Leibniz Institute for Natural Product Research and Infection Biology—Hans Knöll Institute (HKI), Jena, Germany; Department of Microbiology and Molecular Biology, Institute of Microbiology, Friedrich Schiller University Jena, Jena, Germany[e]; Department of Clinical Microbiology and Immunology, Aspergillus and Antifungal Research Laboratory, Sackler School of Medicine, Tel-Aviv University, Ramat-Aviv, Tel-Aviv, Israel[f]; Integrated Research Treatment-Center, Center for Sepsis Control and Care (CSCC), University Hospital Jena, Germany[g]

***Aspergillus fumigatus* is an opportunistic, airborne pathogen that causes invasive aspergillosis in immunocompromised patients. During the infection process, *A. fumigatus* is challenged by hypoxic microenvironments occurring in inflammatory, necrotic tissue. To gain further insights into the adaptation mechanism, *A. fumigatus* was cultivated in an oxygen-controlled chemostat under hypoxic and normoxic conditions. Transcriptome analysis revealed a significant increase in transcripts associated with cell wall polysaccharide metabolism, amino acid and metal ion transport, nitrogen metabolism, and glycolysis. A concomitant reduction in transcript levels was observed with cellular trafficking and G-protein-coupled signaling. To learn more about the functional roles of hypoxia-induced transcripts, we deleted *A. fumigatus* genes putatively involved in reactive nitrogen species detoxification (*fhpA*), NAD^+ regeneration (*frdA* and *osmA*), nitrogen metabolism (*niaD* and *niiA*), and respiration (*rcfB*). We show that the nitric oxygen (NO)-detoxifying flavohemoprotein gene *fhpA* is strongly induced by hypoxia independent of the nitrogen source but is dispensable for hypoxic survival. By deleting the nitrate reductase gene *niaD*, the nitrite reductase gene *niiA*, and the two fumarate reductase genes *frdA* and *osmA*, we found that alternative electron acceptors, such as nitrate and fumarate, do not have a significant impact on growth of *A. fumigatus* during hypoxia, but functional mitochondrial respiratory chain complexes are essential under these conditions. Inhibition studies indicated that primarily complexes III and IV play a crucial role in the hypoxic growth of *A. fumigatus*.**

Aspergillus fumigatus is a ubiquitously distributed saprophytic fungus mainly found in the soil, where it plays an essential role in the degradation of organic debris (1, 2). The fungus propagates by formation of conidia, which easily disperse into the air. During daily life, humans inhale hundreds of *A. fumigatus* conidia, which are efficiently eliminated by the host immune system (3, 4). However, in immunocompromised patients, conidia are able to germinate and grow, eventually leading to an invasive infection called invasive aspergillosis (IA). Due to a rising number of immunodeficient patients, the number of cases of invasive aspergillosis has increased in the last decades. The diagnosis of IA is still difficult, and thus, mortality rates are unacceptably high, ranging from 50 to 90% (5). In addition to these clinical aspects of this disease, the pathophysiology of *A. fumigatus* infections is insufficiently understood. To date, no classic virulence factor has been identified for *A. fumigatus*, and consequently, the adaptation mechanisms of *A. fumigatus* toward the host environment have become a main focus of research.

During infection, long-term low-oxygen conditions challenge this obligate aerobic fungus: O_2 levels drop from 21% in the atmosphere to 14% in the lung alveoli (6). In the surrounding tissue, oxygen availability is further reduced to 2 to 4% and in inflammatory tissue to even less than 1% (7). Such growth conditions were proposed to shape the pathobiology of *A. fumigatus*, and their *in vivo* relevance was further supported by a hypoxia-sensitive mutant (Δ*srbA*) strain, which was avirulent in a mouse model of invasive aspergillosis (8, 9). However, the metabolic response of *A. fumigatus* to hypoxia is less well understood (10). The role of fermentation during hypoxic growth remains ambiguous, and the electron transport chain (ETC) is still active at low oxygen levels for energy production (11). This was also shown in a previous report on hypoxia-induced changes of the transcriptome and proteome in *A. fumigatus* over a period of 24 h (here defined as a short-term response) (12). In this work, the authors used a batch cultivation and monitored the *A. fumigatus* hypoxic response at the time points 2, 6, 12, and 24 h. In a recent proteomic study from our group on the long-term response (5 to 6 days) to hypoxia, *A. fumigatus* was cultivated in an oxygen-controlled chemostat. Under these conditions, an increased abundance of all mitochondrial respiratory chain complexes, especially complex III and IV, was observed (13). In the same study, activation of nitric oxide (NO)-detoxifying enzymes was detected. There is some indication that complex IV may produce NO under oxygen-limiting conditions,

Received 11 April 2014 **Accepted** 24 July 2014
Published ahead of print 1 August 2014
Address correspondence to Olaf Kniemeyer, olaf.kniemeyer@hki-jena.de.
K.K. and V.P. contributed equally to this article.
Supplemental material for this article may be found at http://dx.doi.org/10.1128/EC.00084-14.

doi:10.1128/EC.00084-14

as shown in baker's yeast (14). The increased levels of NO cause posttranslational modifications of proteins (e.g., nitrotyrosination), which may lead to the induction of hypoxic genes (15). Hence, it is supposed that the mitochondrial electron transport chain plays a role in oxygen sensing and hypoxic signaling (16, 17).

However, when the terminal electron acceptor oxygen is limited, many organisms switch from respiration to fermentation to regenerate NAD^+ and to maintain ATP synthesis. Several examples of such alternative electron sinks have already been described in diverse fungal species. In *Aspergillus oryzae* and *Aspergillus nidulans*, genes involved in ethanol fermentation are induced during hypoxic growth conditions (18). However, for *A. fumigatus* no growth phenotype was observed under oxygen-limiting conditions for strains devoid of ethanol fermentation (19). The γ-aminobutyric acid (GABA) shunt pathway has also been proposed to bypass the accumulation of NADH in *A. fumigatus* and *A. nidulans* during hypoxic growth (12, 20, 21). Furthermore, in *A. nidulans* and *Fusarium oxysporum*, growth under oxygen-limiting conditions is supported by using nitrate as an alternative electron acceptor, a process also referred to as ammonia fermentation (22, 23). Taken together, filamentous fungi possess a broad range of metabolic pathways to maintain energy levels under oxygen-limiting conditions, but so far their physiological impact on *A. fumigatus* during hypoxia has remained largely unexplored.

In our previous, aforementioned proteomic study, we established an oxygen-controlled, glucose-limited chemostat as a model for highly reproducible hypoxic cultivations of *A. fumigatus* (13). A follow-up proteomic study on the short-term response of *A. fumigatus* to hypoxia (2 to 24 h) revealed a surprisingly low correlation between the proteomic data of the two studies (12). This may be explained by the different incubation times (6 days versus 2 to 24 h) or culture conditions (glucose-limited chemostat versus batch culture without glucose limitation). To provide further insights into the long-term adaptation mechanism of *A. fumigatus* toward hypoxia, we cultivated *A. fumigatus* under either normoxic (21% partial O_2 pressure [pO_2]) or hypoxic (0.21% pO_2) conditions as described by Vödisch et al. (13) and compared the underlying changes in the transcriptome by microarray analysis. Gene expression at the mRNA level correlated well with our previous proteome data (13) but also suggested an important role for alternative NAD^+-regenerating systems and hypoxic NO signaling. Inhibition of the underlying pathways by gene deletion revealed that alternative electron acceptors, such as nitrate and fumarate, do not have a significant impact on growth during hypoxia in *A. fumigatus*, whereas functional mitochondrial respiratory chain complexes are essential under these conditions.

MATERIALS AND METHODS

Strain and culture conditions. *A. fumigatus* was grown in *Aspergillus* minimal medium (AMM) as previously described (24), containing 60 mM glucose and 70 mM $NaNO_3$ as the sole carbon and nitrogen sources, respectively. To study the long-term response of *A. fumigatus* to hypoxic growth conditions, *A. fumigatus* strain ATCC 46645 was grown in a glucose-limited oxystat (a chemostat with constant oxygen partial pressure) in a continuous culture as described previously by Vödisch et al. (13). Batch fermentation was used to analyze the short-term response of *A. fumigatus* to hypoxic growth conditions. Fermentation was carried out as described previously (12). For expression analysis of the flavohemoprotein *fhpA* gene, either 70 mM $NaNO_3$ or 20 mM L-glutamine was used as the nitrogen source in batch cultivations of *A. fumigatus*. All strains used in this study are listed in Table S1 in the supplemental material.

RNA preparation and transcriptome analysis. For microarray analyses, total RNA was isolated from three independent chemostat cultures, grown under either normoxic or hypoxic conditions. Frozen mycelium of *A. fumigatus* ATCC 46645 was ground to a fine powder, and 100 mg was used for total RNA isolation using the Qiagen RNeasy minikit according to the manufacturer's instructions. Following DNase treatment (TurboDNA-free kit; Ambion, Germany), the quantity and quality of RNA preparations were determined spectrophotometrically with a NanoDrop spectrophotometer (Thermo Fisher Scientific, Germany).

Full-genome transcriptomic analyses were performed at Febit (Heidelberg, Germany) as described previously by Gehrke et al. (25). Briefly, custom-made Geniom biochips comprising ~15,000 oligonucleotide probes were designed, covering the expected number of transcripts based on previous genomic sequence data (26). All data analyses of the FEBIT microarrays were performed using LIMMA (Linear Models for Microarray Data) packages (27) of the Bioconductor software (28). Background correction was performed using the intensities of blank probes, which consist of only a single "T" nucleotide. The median background intensity was subtracted from spot intensity. After conversion of any negative values to a low positive value, signal intensities were $\log_2$ transformed, and duplicate spots were averaged. The obtained data were processed using quantile normalization. To obtain the genes with the most evidence of differential expression, a linear model fit was applied for each gene using LIMMA. Candidate genes for further analysis were selected on the basis of their fold change (≥2) and *P* value (≤0.05).

Nucleic acid hybridizations. Gene deletions were verified by Southern hybidizations. Briefly, genomic DNA of *A. fumigatus* was extracted using the MasterPure yeast DNA purification kit (Epicentre Biotechnologies) and digested by specific restriction enzymes (New England BioLabs, Germany). Resulting DNA fragments were separated by agarose gel (1% [wt/vol]) electrophoresis and transferred onto Hybond-N^+ membranes (GE Healthcare Bio-Sciences, Germany) by capillary blotting. Gene-specific DNA probes were generated by PCR, including digoxigenin (DIG)-labeled dUTPs (Jena Bioscience, Germany) or [α-^{32}P]dCTP (Institute of Isotopes C, Ltd., Hungary). DIG-labeled probes were hybridized with DIG Easy Hyb and detected using antidigoxigenin antibodies and CDP-Star as an ultrasensitive fluorescent substrate of alkaline phosphatase (Roche Applied Science, Germany). Oligonucleotides used for amplifying labeled DNA probes are shown in Table S2 in the supplemental material. For Northern hybridizations, 10 μg of total RNA was separated on a denaturing agarose gel (1.2% [wt/vol] agarose, 40 mM morpholinepropanesulfonic acid [MOPS], 10 mM sodium acetate, 2 mM EDTA, 2% [vol/vol] formaldehyde [pH 7]). Blotting, hybridization, and detection were done as described above. The primers used to generate mRNA-specific DNA probes are listed in Table S3 in the supplemental material.

Generation of fungal strains. *A. fumigatus* CEA17Δ*akuB*^{KU80} (29) mutants were generated by homologous recombination following the transformation of protoplasts (30). All mutant strains used in this study are listed in Table S1 in the supplemental material.

For deletion of the fumarate reductase *frdA* (locus tag no. AFUA_7G05070; http://www.aspgd.org), the flanking regions were amplified from genomic DNA with the primer pairs FrdA_LF_fw/FrdA_LFhph_rev and FrdA_RFhph_fw/FrdA_RF_rev. This reaction produces overlapping ends to the hygromycin resistance cassette at the 3′ end of the upstream flanking region and at the 5′ end of the downstream flanking region of the *frdA* gene. The hygromycin resistance cassette was amplified from plasmid pUChph (31) using the primers Hph_fw and Hph_rev. The *frdA* deletion construct was obtained by a 3-fragment PCR using the primers FrdA_LF_fw and FrdA_RF_rev. Similarly, the SREBP transcription factor *srbA* (AFUA_2G01260) was deleted by amplifying the corresponding flanking region using the primers SrbA_LF_fw/SrbA_LFhph_rev and SrbA_RFhph_fw/SrbA_RF_rev.

For deletion of the fumarate reductase *osmA* (AFUA_8G05530), the nitrate reductase *niaD* (AFUA_1G12830), and the nitrite reductase *niiA* (AFUA_1G12840) genes, the corresponding flanking regions were ampli-

fied using the primer pairs OsmA_LF_fw/OsmA_LFptrA_rev and OsmA_RFptrA_fw/OsmA_RF_rev, NiaD_LF-fw/NiaD_LFptrA_rev and NiaD_RFptrA-fw/NiaD_RF_rev, and NiiA_LF-fw/NiiA_LFptrA_rev and NiiA_RFptrA-fw/NiiA_RF_rev, respectively. Here, pyrithiamine resistance was used as the selection marker, and the respective gene was amplified from plasmid pSK275 (32) using the primers PtrA_fw and PtrA_rev.

For the generation of the Δ*frdA* Δ*osmA* double knockout strain, the *osmA* deletion cassette containing pyrithiamine resistance (as described above) was used to transform the Δ*frdA* strain. Transformants were selected on AMM plates containing either 0.1 μg/ml pyrithiamine (Sigma, Germany) or 240 μg/ml hygromycin (Roche Applied Science, Germany).

To generate a C-terminal enhanced green fluorescent protein (eGFP) fusion protein with the flavohemoprotein FhpA (AFUA_4G03410), 1 kb of the native promoter and the *fhpA* gene were amplified from genomic DNA of *A. fumigatus* CEA17Δ*akuB*^{KU80} using the primers FhpA_GFP_HindIII_fw and FhpA_GFP_BamHI_rev. The obtained DNA fragment was inserted into the vector p123_eGFP (33) containing the hygromycin resistance cassette. The resulting vector, pfhpA_egfp, was ectopically integrated into the genome of *A. fumigatus* CEA17Δ*akuB*^{KU80} Δ*fhpA* (derived from M. Vödisch [unpublished data]).

All PCRs were performed with Phusion high-fidelity DNA polymerase (Thermo Fisher Scientific, Germany) according to the manufacturer's recommendations. All oligonucleotides used for the generation of mutant strains are listed in Table S2 in the supplemental material.

The deletion construct for *rcfB* (AFUA_1G12250) was prepared using the yeast recombinational cloning technique (34). Primers were designed and synthesized with the 5′ common regions highlighted in italic in Table S2 in the supplemental material. The hygromycin cassette (*Hph*), containing 5′ and 3′ HindIII and XbaI restriction sites, was generated by PCR amplification using the primers Hph 5′ and Hph 3′. Yeast shuttle vector pYes2 was digested with HindIII and XbaI. Yeast strain BY4741 was used for yeast transformation following the protocol described by Collopy et al. (34). Yeast DNA was prepared with the Masterpure yeast DNA purification kit (Epicentre Biotechnologies). Transformation of *A. fumigatus* CEA17Δ*akuB*^{KU80} protoplasts with linearized plasmids (Δ*Afu1g12250-Hph*) (EcoRV) was carried out as previously described (35).

Growth susceptibility assays. Conidia were harvested after 5 days of cultivation on AMM agar plates with sterile water and filtered through a 40-μm-pore cell strainer (BD Biosciences, Germany). Conidia were serially diluted in sterile water to obtain defined concentrations and 10^5, 10^4, 10^3, and 10^2 conidia were spotted in a volume of 5 μl on AMM agar plates in the presence of certain stress-inducing agents. Growth was documented after 48 or 72 h of incubation at 37°C.

To generate nitrosative stress conditions, different concentrations of sodium nitrite were added in acidified AMM (pH 4.5). Reductive stress conditions were induced by the addition of 10 mM tris(2-chloroethyl) phosphate (TCEP)-HCl (final concentration).

Normoxic or two hypoxic atmospheres consisting of either 1% O_2 and 5% CO_2 (HeraCell 150, Thermo Fisher Scientific, Germany) or 0.2% O_2 and 5% CO_2 (H35 Hypoxystation; Don Whitley Scientific, United Kingdom) were used to monitor growth of *A. fumigatus* on AMM agar plates.

A. fumigatus wild-type strain and the hypoxia-sensitive Δ*srbA* strain were cultivated in the presence of specific respiratory chain inhibitors (Sigma-Aldrich, Germany): 1, 2, 3, and 4 mM rotenone (complex I inhibitor); 50, 75, 100, and 150 μM flavone (inhibitor of alternative NADH: ubiquinone oxidoreductases); 100, 200, 300, 400, and 500 mM disodium malonate (complex II inhibitor); 5, 10, and 20 μM antimycin A (complex III inhibitor); 0.25, 0.5, and 1 mM sodium azide (complex IV inhibitor); 5, 10, and 20 μM oligomycin (complex V inhibitor); 0.5, 1, and 2 mM 2,4-dinitrophenole (transmembrane H^+ carrier inhibitor); and 2.5, 5, and 10 mM salicylhydrosamic acid (alternative oxidase inhibitor). Five-microliter aliquots of each strain were spotted in 10-fold serial dilutions on AMM agar plates containing the respective inhibitor at the concentrations indicated above.

Reductive stress assay. To monitor growth in the presence of the reductive stress agent TCEP-HCl (Merck KGaA, Germany) in liquid culture (96-well microtiter plate [96 MTP] format), 2,000 conidia were inoculated per well, containing AMM supplemented with 0 to 20 mM TCEP-HCl. The plate was incubated for 3 days at 37°C, and growth was documented.

Determination of succinic acid concentration. The concentration of succinic acid in the culture supernatant was quantified with an enzymatic detection kit according to the manufacturer's instructions (UV test for succinic acid; R-Biopharm, Germany).

Fluorescence microscopy studies. For fluorescence imaging, 50 μl AMM (containing either nitrate [70 mM] or glutamine [20 mM] as the nitrogen source) was inoculated with 1×10^4 conidia of an FhpA-eGFP strain on glass coverslips in a wet chamber. After 14 h of precultivation under normoxic conditions at 37°C, samples were shifted to a hypoxic atmosphere with 1% O_2 and 5% CO_2 at 37°C (HeraCell 150; Thermo Fisher Scientific, Germany). Samples were analyzed after 0, 3, 6, 12, and 24 h of hypoxia using a Leica DMI 4000B fluorescence microscope (Leica Microsystems, Germany). Images were taken with a Leica DFC480 camera and analyzed by Leica LAS V.3.7 software.

Egg infection model. Virulence of *A. fumigatus* CEA17Δ*akuB*^{KU80} and the Δ*frdA*, Δ*osmA*, Δ*frdA* Δ*osmA*, and Δ*niiA* deletion strains was tested in an established egg model for *Aspergillus* species (36). Briefly, after 7 days of cultivation on malt agar plates at room temperature, conidia were harvested in phosphate-buffered saline (PBS) containing 0.1% Tween 20 (vol/vol) and filtered with a 40-μm-pore cell strainer (BD Bioscience, Germany). After counting of conidia by using either a counting chamber (Roth, Germany) or the CASY cell counter analyzer TT (Roche Applied Science, Germany), conidia were diluted with PBS to a concentration of 10^4 conidia/ml just prior to infection. PBS alone was used as a negative control. Embryonated eggs were incubated at 37.6°C and 50 to 60% relative humidity (BSS 300; Grumbach, Germany). After 10 days of incubation, 20 eggs per group were infected with 10^3 conidia/egg via the chorioallantoic membrane (CAM), and survival was monitored daily over 7 days by candling. Survival data were plotted as Kaplan-Meyer curves and statistically analyzed by a log rank test using Graph Pad Prism 5.00 (GraphPad Software).

Statistics. The Student *t* test was used for significance testing of two groups. Differences between the groups were considered significant at $P \leq 0.05$ or $P \leq 0.01$.

Microarray data accession number. Data from the microarray analyses have been deposited in the OmniFung Data Warehouse (http://www.omnifung.hki-jena.de) and ArrayExpress (accession no. E-MTAB-2699). These data can be easily accessed by public login.

RESULTS

Gene expression in long-term hypoxia-adapted *A. fumigatus*. To study the effect of long-term exposure to hypoxia on the transcriptional profile of *A. fumigatus*, we cultivated the fungus in a chemostat, which allowed us to vary the oxygen partial pressure (21% pO_2 and 0.21% pO_2), while all other cultivation parameters such as glucose concentration, pH, and temperature were kept constant. A dilution rate of 0.08 h^{-1} was applied to ensure the same growth rate under normoxic and hypoxic conditions. Steady-state growth was reached after between 3 to 4 days and the biomass of 750 mg dry weight $liter^{-1}$ was harvested after 5 to 6 days followed by RNA extraction.

Febit Geniom biochips representing 15,000 open reading frames were hybridized with RNA from three replicates of each sample. We applied a principle component analysis method (Sammon's nonlinear mapping) to determine sample variance and to identify outliers. One sample outlier (0.21% O_2) was detected, which was excluded from further analysis. Genes showing at least 2-fold changes in expression ($P \leq 0.05$) were considered to be differentially expressed.

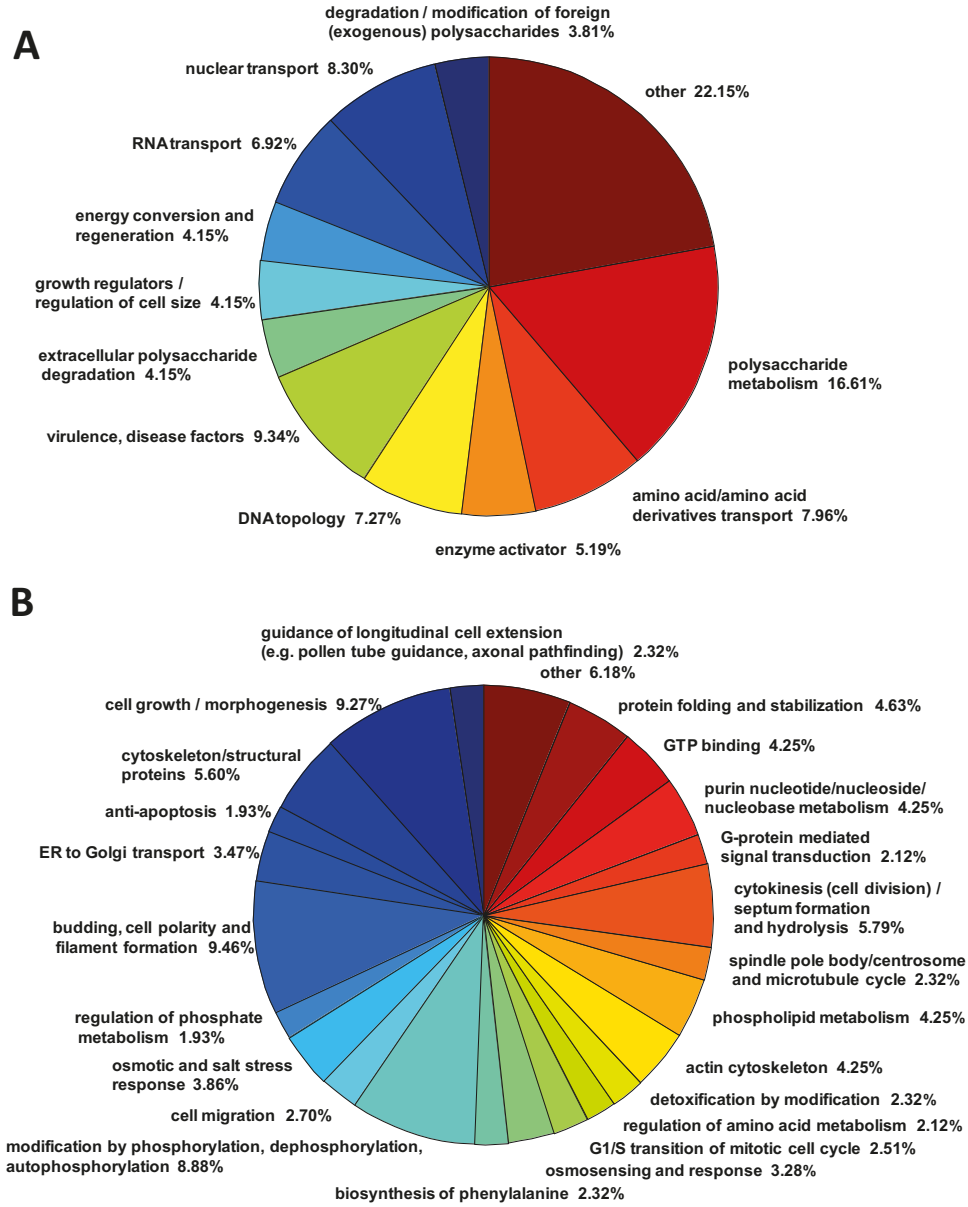

FIG 1 Gene set enrichment (GSE) analysis of upregulated (A) and downregulated (B) genes during long-term exposure of *A. fumigatus* to hypoxia based on FunCat classification.

In total, 1,614 genes were upregulated and 1,260 genes were significantly downregulated in *A. fumigatus* during growth under hypoxia in a glucose-limited chemostat (see Data Set S1 in the supplemental material). Gene set enrichment (GSE) analysis based on FunCat and Gene Ontology (GO) classification was performed to gain a general overview of the type of categories affected by hypoxia (Fig. 1; see Fig. S1 in the supplemental material). Specific categories of transcripts that were significantly upregulated under hypoxia were associated with nuclear and RNA transport, energy conversion, polysaccharide degradation, DNA topology, enzyme activation, amino acid, metal ion, and transmembrane transport, nitrogen compound and metabolic processes, the glyoxylate cycle, gluconeogenesis, and methionine biosynthesis. Furthermore, several flavin-containing enzymes involved in oxidation reduction processes were also upregulated. As expected, many additional metabolic changes occurred in response to hypoxia. Many glycolytic gene transcripts and several transcripts related to ethanol fermentation showed higher mRNA abundance in hypoxia: a pyruvate decarboxylase gene (AFUA_3G11070) along with two alcohol dehydrogenase genes, *alcC* (AFUA_5G06240) and *adh2* (AFUA_2G10960). In agreement with previous findings from other fungi that the GABA shunt could reduce NADH accumulation at low oxygen levels, we found transcription of the succinate-semialdehyde dehydrogenase gene (AFUA_3G07150) to be significantly higher in response to hypoxia. Considering transcription factors, transcript levels of the central regulator of hypoxia adaptation, SrbA (AFUA_2G01260), was also activated as the mRNA of this transcription factor was increased 4.9-fold, which

in turn activated key enzymes of sterol metabolism. An increased need for iron under hypoxia is illustrated by the fact that the iron regulator HapX (AFUA_5G03920) was slightly upregulated (1.2-fold), whereas the repressor of iron acquisition, SreA (AFUA_5G11260), showed lower transcript levels (−2.8) under hypoxia.

Other FunCat categories were significantly reduced in response to hypoxia and include, among others, cytoskeleton/structural proteins, endoplasmic reticulum (ER)-to-Golgi transport, modification by phosphorylation, osmosensing and response, cell redox homeostasis, phospholipid metabolism, and G-protein-mediated transduction. Presumably, in hypoxia-grown cells there is a reduction in cellular trafficking and signaling activity via G-protein-coupled receptors and small GTPases.

When comparing these gene expression data to the hypoxia proteome from our previous study (13), we found a good correlation. Two-thirds of the proteins (44 out of 66) showed the same tendency of regulation as their corresponding transcript (see Table S4 in the supplemental material). An opposite change in abundance was observed for a few glycolytic enzymes, antioxidative proteins, enzymes of the tricarboxylic acid (TCA) cycle, and the electron transport chain, which suggests a regulation of these proteins at the posttranscriptional level.

A comparison with the transcriptome data from the hypoxic response of *A. fumigatus* cultivated in a batch fermenter at low oxygen levels for 24 h by Barker et al. (12) revealed that only 27% of the 867 significantly altered genes were also differentially expressed in our study (see Fig. S2 in the supplemental material). These transcripts included genes involved in metabolic processes, such as amino acid, lipid, and terpenoid biosynthesis, and cofactor and nucleotide metabolism, as well as replication, cellular transport processes, and protein folding/modifications. The biggest differences were seen in the FunCat categories transcription and protein synthesis. Transcription levels of genes involved in these processes decreased only significantly in the study of Barker et al. (12). This suggests that transcription and translation are only transiently downregulated during hypoxia.

Confirmation of microarray data by Northern blotting analyses. To confirm the robustness and quality of our transcriptome data from *A. fumigatus* cultivated in an oxygen-controlled chemostat, we analyzed the gene expression of five selected genes during hypoxia by Northern hybridization (Fig. 2). These included genes involved in reactive nitrogen species detoxification (*fhpA* [AFUA_4G03410]), NAD^+ regeneration (*frdA* [AFUA_7G05070]), nitrogen metabolism (*niiA* [AFUA_1G12840]), and respiration (*cox5b* [AFUA_2G03010] and *rcfB* [AFUA_1G12250]). Hereby, RNA samples produced for our microarray experiment were used.

The microarray data revealed a 17-fold upregulation of the flavohemoprotein-encoding gene *fhpA*, which was also confirmed by Northern blotting (Fig. 2). This result is consistent with the proteome analysis of both long- and short-term responses of *A. fumigatus* under hypoxic growth conditions (12, 13). Another interesting finding of the microarray study was the drastically increased expression (321-fold upregulation) of the cytosolic fumarate reductase gene *frdA*, which was also verified by Northern hybridizations (Fig. 2). For the gene *osmA*, which encodes the fumarate reductase isoenzyme OsmA (AFUA_8G05530), the extent of induction was by more than one order of magnitude lower. However, Northern blot analysis revealed no clear difference in the expression level of *osmA* during normoxia and hypoxia (Fig. 2).

In addition, the microarray data revealed, that several transcripts linked to nitrate metabolism were significantly increased (Table 1). Among them, the nitrite reductase *niiA* transcript showed the highest increase in expression level. However, Northern blot analyses revealed only a slight increase in *niiA* mRNA steady-state levels and no altered expression of nitrate reductase *niaD* during hypoxic growth conditions (Fig. 2).

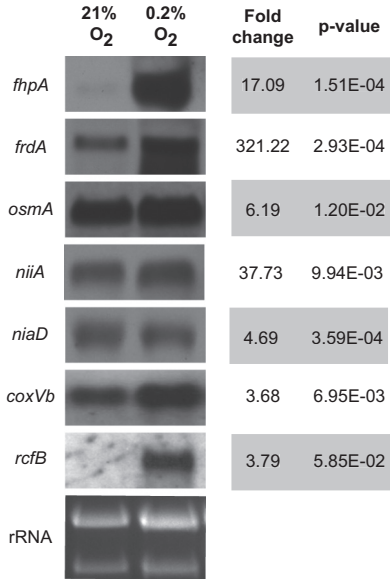

FIG 2 Confirmation of the expression of hypoxia-induced transcripts during cultivation of *A. fumigatus* in an oxygen-controlled chemostat by Northern blotting. *A. fumigatus* was cultivated in a continuous culture under either normoxic or hypoxic conditions for 6 days. (Left panel) Northern hybridizations of upregulated genes. RNA was isolated from normoxic and hypoxic samples. Ten micrograms of RNA was loaded per lane. rRNA bands are displayed as a loading control. (Right panel) Microarray fold changes and *P* value of the corresponding genes.

Interestingly, two components of the cytochrome *c*-oxidase respiratory complex, which acts as the terminal enzyme of the respiratory chain, were also expressed at significantly higher levels during hypoxia. This was subsequently confirmed by Northern hybridizations as well (Fig. 2). These two genes encode the integral subunit CoxVb and an Rcf2-like protein, here named RcfB. The orthologous gene from *S. cerevisiae* was also reported to be highly upregulated under hypoxia (37, 38). The other known respiratory supercomplex factor similar to RcfB, RcfA (AfuA_4G08130), was not significantly upregulated under our experimental hypoxic conditions.

Taken together, these data prompted us to analyze the impact

TABLE 1 Overview of the upregulated transcripts dealing with nitrate metabolism

Product description	Locus tag no.	Ratio	*P* value
Nitrate reductase NiaD	AFUA_1G12830	+4.69	0.000359
Nitrite reductase NiiA	AFUA_1G12840	+37.73	0.00994
Nitrate transporter CrnA	AFUA_1G12850	+6.2	0.013
High-affinity nitrate transporter NrtB	AFUA_1G17470	+6.28	0.0923
Periplasmic nitrate reductase	AFUA_3G15190	+4.29	0.00952
Nitrate reductase	AFUA_5G10420	+2.83	0.00242
Multicopper oxidase	AFUA_3G14950	+19.46	0.0303

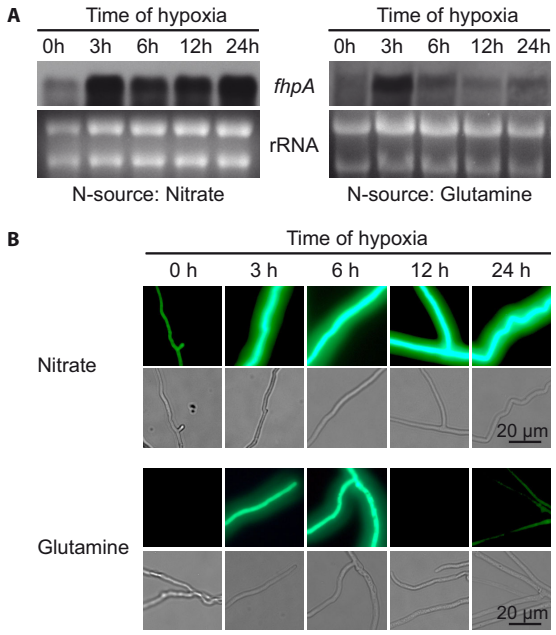

FIG 3 Regulation of flavohemoprotein *fhpA* during hypoxic growth conditions in dependence of the nitrogen source. (A) Northern blot analysis of *fhpA*. *A. fumigatus* ATCC 46645 was cultivated under hypoxia in batch fermentation using nitrate or glutamine as the nitrogen source. RNA was isolated from samples taken after 0, 3, 6, 12, and 24 h of hypoxia, and 10 μg was loaded per lane. rRNA bands are displayed as a loading control. (B) Fluorescence studies of the FhpA-eGFP fusion strain. The *A. fumigatus* FhpA-eGFP strain was cultivated in AMM containing nitrate or glutamine as the nitrogen source. After 14 h of precultivation under normoxic conditions, cultures were incubated for a further 24 h at 1% O_2. Using a constant exposure time, fluorescence signals were monitored after 0, 3, 6, 12, and 24 h of hypoxia. The size bar represents 20 μm.

of NO detoxification, NAD^+ regeneration, and respiration on the hypoxic adaptation of *A. fumigatus* in more detail.

Nitrate-independent induction of the flavohemoprotein FhpA during hypoxia. To elucidate the role of the flavohemoprotein FhpA during hypoxia, we characterized its regulation in more detail. In aspergilli, the NO dioxygenase activity of flavohemoproteins suggests a role in the detoxification of nitric oxide (NO), which is formed during nitrate assimilation (39, 40). In agreement, it was shown that *fhpA* is expressed in the presence of nitrate but repressed when glutamine is used as sole nitrogen source (K. Lapp, M. Vödisch, K. Kroll, M. Strassburger, O. Kniemeyer, T. Heinekamp, and A. A. Brakhage, unpublished data). This raises the question of whether the observed upregulation of *fhpA* was induced by hypoxia or by the nitrate assimilation process. Thus, *A. fumigatus* was cultivated after 14 h of normoxic precultivation under hypoxic batch fermentation for 24 h, using either nitrate or glutamine as the sole nitrogen source. Subsequently, the expression of *fhpA* was monitored over time (Fig. 3A). In the presence of nitrate, the hypoxia-induced expression of *fhpA* remained constant over time. In contrast, when using glutamine as a nitrogen source, the expression levels of *fhpA* increased after 3 h of hypoxia but dropped to their original level after longer periods of oxygen depletion. Therefore, we conclude that nitrate promotes a stronger and longer-lasting induction of *fhpA* expression under hypoxia than glutamine. These results were further confirmed by expression analysis of a FhpA-eGFP fusion protein in an *A. fumigatus* strain cultivated under similar conditions (Fig. 3B; see Fig. S3 in the supplemental material). This suggests that the expression of the flavohemoprotein gene *fhpA* is induced by hypoxia independently of the nitrogen source, whereas the duration of expression is depending on it. The contribution of FhpA to the hypoxic survival of *A. fumigatus* was tested by cultivating an Δ*fhpA* deletion (unpublished data) strain under hypoxic (0.2% O_2) and normoxic (21% O_2) conditions with either nitrate or glutamine as nitrogen source. However, the Δ*fhpA* strain showed a wild-type growth phenotype under hypoxic conditions.

Nitrate metabolism during hypoxia. Under anoxic conditions, a variety of bacteria and fungi, such as *Bacillus subtilis*, *Escherichia coli*, or *F. oxysporum* are able to use alternative terminal electron acceptors (41–45). Among them, nitrate (NO_3^-/NO_2^-) with a relatively high redox potential, ($E'_0 = +0.42$ V) is the most efficient electron acceptor besides oxygen ($E'_0 = +0.82$ V).

However, no dissimilatory nitrate reduction has been reported for *A. fumigatus*. The fungus assimilates nitrate via nitrite (NO_2^-) reduction to ammonium (NH_4^+). These reactions are catalyzed by the NADPH-dependent assimilatory nitrate and nitrite reductases, NiaD (AFUA_1G12830) and NiiA (AFUA_1G12840), respectively. Whether this pathway may serve as alternative electron sink during hypoxia in *A. fumigatus* has not been shown yet.

To study the impact of these two enzymes on the adaptation to hypoxia, we generated the corresponding Δ*niaD* and Δ*niiA* deletion mutants (see Fig. S4A and B in the supplemental material). As expected, lack of *niaD* or *niiA* abolished growth when nitrate was used as sole nitrogen source (data not shown). Surprisingly, in the presence of other primary nitrogen sources, such as glutamine or ammonium tartrate, growth of the Δ*niiA* strain was also slightly reduced compared to that of the wild type and the Δ*niaD* strain (see Fig. S4C). However, no altered growth phenotype of the mutants was observed under hypoxic conditions (see Fig. S4C), which confirmed that these assimilatory enzymes are not linked to respiratory nitrate ammonification in *A. fumigatus* during hypoxic growth conditions. More likely, these enzymes may be involved in nitric oxide intermediate (RNI) detoxification. It has been shown, that the mitochondrial cytochrome *c* oxidase Cco can produce NO by reducing NO_2^- under oxygen-limiting conditions (14, 46–49). To test whether the increased expression of *niaD* and *niiA* were caused by NO formation during hypoxia, the Δ*niaD* and Δ*niiA* strains and the corresponding wild-type strain CEA17Δ*akuB*^{KU80} were cultivated in the presence of sodium nitrite, which decomposes spontaneously to nitric oxide at an acidic pH of 4.5 (50) (Fig. 4). Resistance toward NO of the Δ*niaD* strain was similar to the wild type, whereas growth of the Δ*niiA* strain was visibly impaired (Fig. 4). However, agar diffusion assays with the NO donor diethylenetriamine (DETA)-NO (data not shown) revealed no difference in sensitivities between the Δ*niiA* and wild-type strains. Taken together, these data suggest that the nitrite reductase NiiA is only indirectly involved in the adaptation to hypoxic growth conditions. Its role in detoxifying harmful RNIs during hypoxia remains unclear. Its slight upregulation under these conditions may also simply be explained by a coregulation with FhpA as reported from *A. nidulans* (40).

To analyze the impact of *niiA* on virulence, embryonated eggs were infected with spores of the Δ*niiA* strain. However, no significant differences in survival were observed between embryonated eggs infected with the mutant and those infected with the corre-

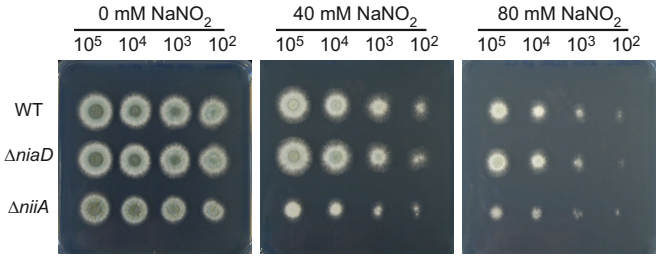

FIG 4 Growth of nitrate and nitrite reductase deletion strains under nitrosative stress conditions. Five-microliter aliquots of each strain were spotted in a serial 10-fold dilution on AMM agar plates with 20 mM glutamine as the primary nitrogen source and 0, 40, or 80 mM $NaNO_2$ at pH 4.5 to impose nitrosative stress. Growth was documented after 48 h of incubation at 37°C under normoxic conditions.

sponding wild-type strain (see Fig. S5A in the supplemental material).

Fumarate metabolism during hypoxia. Besides nitrate, fumarate represents another alternative electron acceptor in the absence of oxygen. The yeast *Saccharomyces cerevisiae* genome contains two soluble fumarate reductases that are essential for anaerobic growth (51). In *A. fumigatus*, the cytosolic flavin adenine dinucleotide (FAD)-dependent oxidoreductase FrdA (AFUA_7G05070) revealed 43% amino acid identity to the cytosolic fumarate reductase Frd1 in *S. cerevisiae*. The second fumarate reductase of *A. fumigatus*, OsmA (AFUA_8G05530), was 42% identical to the corresponding yeast homologue, which is localized in the promitochondria (51). Remarkably, under hypoxic conditions, fumarate reductase *frdA* represented the gene with the highest induction found in our microarray study. This is in agreement with the increased abundance of FrdA in the proteome of the short-term response of *A. fumigatus* against hypoxia (12).

Next, we examined the time-dependent change of gene expression levels of fumarate reductases *frdA* and *osmA* in more detail during a 24-h period of hypoxia (batch cultivation). Similar to the results of the chemostat, during batch cultivation, expression of *frdA* was induced over all time points tested (Fig. 5A). In contrast, transcript levels of *osmA* were transiently increased within the first 3 h of hypoxia (Fig. 5A). When we quantified the fumarate reductase product succinic acid, we could indeed detect increased concentrations of succinic acid in the culture supernatants of hypoxic batch fermentations. However, during hypoxia the amount of succinic acid increased only slightly over time from 0.04 mM to 0.085 mM and the concentration remained low (Fig. 5B).

To investigate the role of both fumarate reductases during hypoxia in more detail, *frdA* and *osmA* were deleted in *A. fumigatus* (see Fig. S6A and B in the supplemental material), and the growth phenotypes of the obtained Δ*frdA* and Δ*osmA* knockout strains and the Δ*frdA* Δ*osmA* double mutant were further characterized. However, no significant differences were observed in growth between the wild-type and knockout strains under hypoxia (see Fig. S6C and D). In yeast, fumarate reductases are involved in the reoxidation of FAD prosthetic groups of flavoenzymes during anaerobiosis (52). This fits with a slight growth defect of the Δ*frdA*, Δ*osmA*, and Δ*frdA* Δ*osmA* strains in the presence of tris(2-chloroethyl)phosphate (TCEP) (Fig. 5C and D). TCEP reduces disulfide bonds as sufficiently as dithiothreitol (DTT), but in contrast to DTT, it is relatively resistant to air oxidation. All three mutants did not grow in the presence of 20 mM TCEP in liquid AMM,

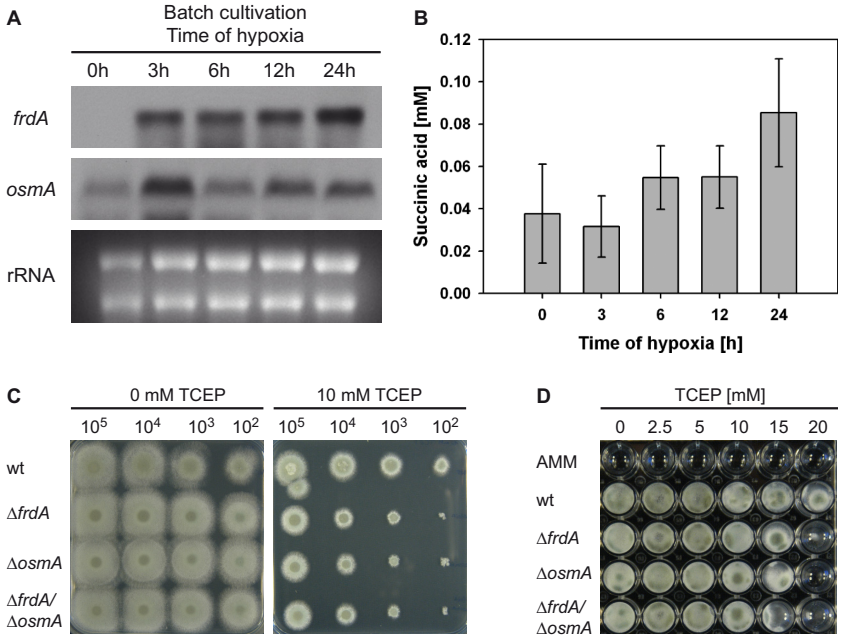

FIG 5 (A and B) Analysis of fumarate respiration during batch cultivation of *A. fumigatus* under hypoxic conditions. *A. fumigatus* CEA17Δ*akuB*^{KU80} was cultivated under hypoxia in batch fermentation. Samples were taken after 0, 3, 6, 12, and 24 h of hypoxia. (A) Northern blot analysis of *frdA* and *osmA*. Ten micrograms of RNA was loaded per lane. rRNA was used as the loading control. (B) Quantification of succinic acid in the supernatant. (C and D) Influence of TCEP on growth of fumarate reductase deletion strains. (C) Five-microliter aliquots of each strain were spotted in a serial 10-fold dilution on AMM agar plates containing 0 or 10 mM TCEP. (D) A total of 2×10^3 condia per well were cultivated in the presence of 0 to 20 mM TCEP. Growth differences were detected after 72 h of incubation at 37°C under normoxic conditions.

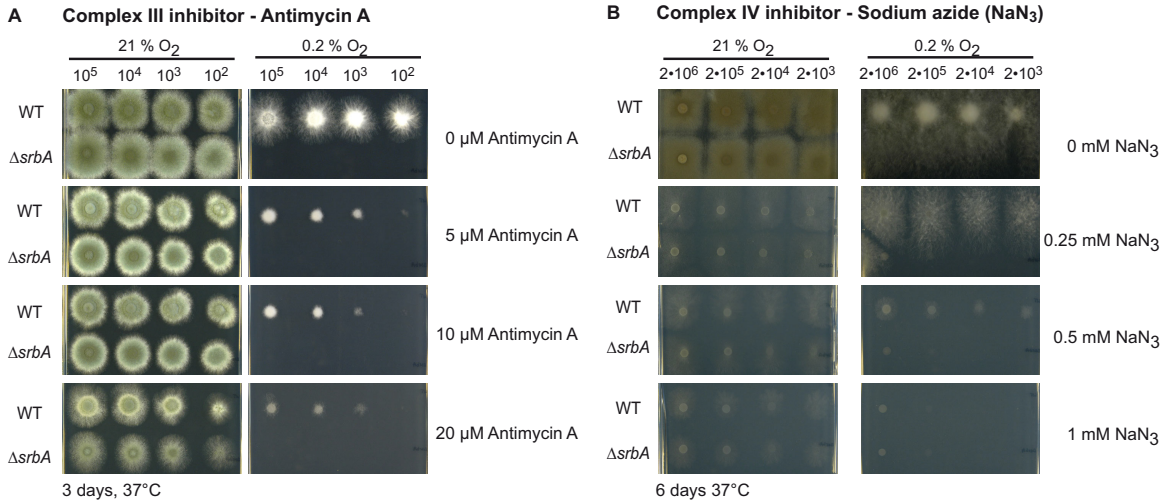

FIG 6 Impact of the inhibition of complexes III and IV on growth of *A. fumigatus* during hypoxia. Five-microliter aliquots of the wild-type and Δ*srbA* strains were spotted in a serial 10-fold dilution on AMM agar plates in the presence of 0 to 20 μM antimycin A (A) and 0 to 1 mM sodium azide (B). Growth differences were detected after 3 or 6 days of incubation at 37°C under normoxic and hypoxic conditions.

whereas the wild type still formed hyphae. Reducing agents such as TCEP induce reductive stress and the unfolded protein response (UPR) in fungal cells. Finally, to analyze any potential impact of fumarate reductases on the virulence of *A. fumigatus*, the Δ*frdA*, Δ*osmA*, and Δ*frdA* Δ*osmA* strains were tested in an embryonated egg infection model. However, no significant differences in virulence between eggs infected with fumarate reductase deletion strains and eggs infected with the wild type were observed, indicating that the enzymes are dispensable for infection in this particular, alternative model (see Fig. S5B in the supplemental material).

Taken together, these data demonstrate that fumarate reductases are unlikely to function as respiratory enzymes but may contribute to regenerate the FAD/flavin mononucleotide (FMN) prosthetic group of flavoenzymes in *A. fumigatus*.

Role of respiratory complexes during hypoxic adaptation. Despite previous indications for fermentation pathways, mitochondrial respiration has proven to be essential during hypoxia (11, 13). To further investigate the robustness of this pathway and the specific contribution of each individual respiratory complex to hypoxic survival, *A. fumigatus* wild-type strain and the hypoxia-sensitive Δ*srbA* strain were cultivated in the presence of specific respiratory chain inhibitors.

Inhibition of complex I by rotenone had no effect on the growth of *A. fumigatus* during normoxia and resulted in only a very slight reduction of growth under hypoxic conditions in a concentration-dependent manner (see Fig. S7A in the supplemental material). When complex I is inhibited, fungi and plants are able to regenerate NAD^+ via alternative NADH:ubiquinone oxidoreductases (53, 54). In turn, inhibition of these alternative NADH dehydrogenases by flavone resulted in a strong growth defect under both normoxic and hypoxic conditions (see Fig. S7B). Even when both inhibitors (rotenone and flavone) of the respiratory NAD^+ regeneration system were combined, *A. fumigatus* was still able to grow in normoxic and hypoxic atmospheres (see Fig. S7C). Similarly, as for complex I, inhibition of the complex II component succinate dehydrogenase by disodium malonate of complex V by oligomycin or of the transmembrane H^+ carrier by 2,4-dinitrophenol resulted in a reduction in fungal growth, which was, however, largely independent of the atmospheric O_2 levels (see Fig. S8 and S9 in the supplemental material).

Hypoxia-specific effects were seen only for complexes III and IV. During normoxia, the lowest applied concentration of the complex III inhibitor antimycin A (5 μM) provoked only a slight inhibitory effect on growth of *A. fumigatus*, but growth was severely impaired when the same concentration was used under hypoxic conditions (Fig. 6A). Similar results were obtained when complex IV was inhibited by sodium azide (Fig. 6B). Under normoxia, growth of *A. fumigatus* was reduced independent of the applied inhibitor concentration. In contrast, under hypoxic conditions sodium azide inhibited growth of *A. fumigatus* in a highly concentration-dependent manner. At a concentration of 0.25 mM sodium azide, the wild type did show a difference in sensitivity between normoxic and hypoxic conditions. This may be explained by a compensatory increased activity of the alternative oxidase (AOX).

Many fungi are equipped with an AOX. It represents a terminal ubiquinol oxidase bypassing complexes III and IV of the electron transport chain (53, 54). The specific AOX inhibitor SHAM reduced growth of the *A. fumigatus* wild type in a concentration-dependent manner under both normoxic and hypoxic conditions (Fig. 7A). Remarkably, the Δ*srbA* mutant strain (see Fig. S10A in the supplemental material), deleted of the hypoxia regulator SrbA, showed poor growth in the presence of SHAM. To investigate this further, Northern blot analysis was performed, which revealed increased expression of *aox* in the Δ*srbA* mutant under normoxic conditions (Fig. 7B). However, for cytochrome *c* (*cycA*), no altered gene expression was observed between the *A. fumigatus* wild-type and Δ*srbA* strains (Fig. 7B). This finding suggests that SrbA is directly or indirectly a negative regulator of the *aox* gene under normoxic conditions.

Taken together, our data indicate that complexes III and IV play an essential role in the adaptation process toward hypoxic growth conditions.

Furthermore, our microarray data suggested that additional factors may contribute to the assembly of respiratory complexes,

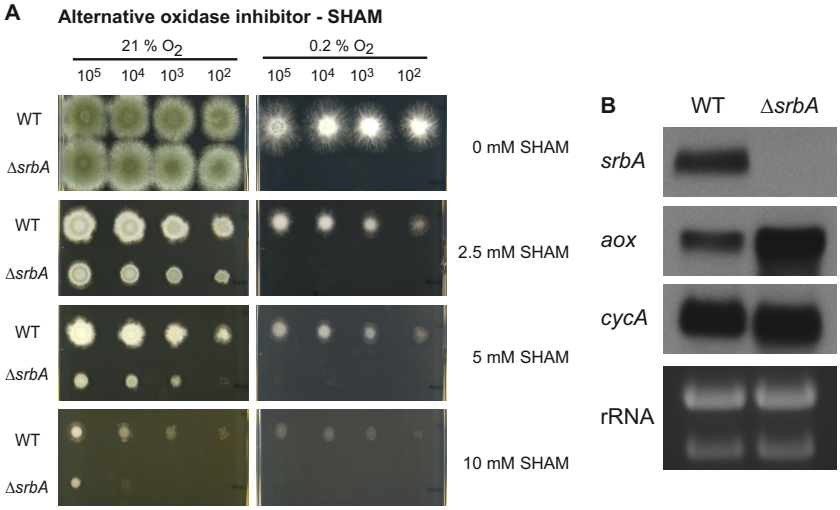

FIG 7 (A) Impact of the inhibition of the alternative oxidase on growth of *A. fumigatus* under hypoxic conditions. Five-microliter aliquots of the wild-type and Δ*srbA* strains were spotted in a serial 10-fold dilutions on AMM agar plates in the presence of SHAM (0 to 10 mM). Growth differences were detected after 3 days of incubation at 37°C under normoxic and hypoxic conditions. (B) Northern blot analysis of the *A. fumigatus* Δ*srbA* strain. A 100-ml volume of AMM was inoculated with 10^8 conidia of the *A. fumigatus* wild-type or Δ*srbA* strain and incubated for 24 h at 37°C and 200 rpm. RNA was isolated, and 10 μg RNA was loaded per lane. rRNA bands are displayed as a loading control.

especially under hypoxic conditions. One candidate gene encodes a protein which comprised a HIG-1 domain (PF04588 [hypoxia-inducible gene]) and revealed amino acids 32% identical to those in the Rcf2 protein from *S. cerevisiae*. In *S. cerevisiae*, Rcf2 and its close homologue, Rcf1, which is essential for hypoxic growth (55), are involved in the assembly of respiratory supercomplexes (37). The hypoxic induction of the corresponding homologue *rcfB* in *A. fumigatus*, prompted us to analyze whether its protein product would also play a vital role in the assembly of these complexes during hypoxic adaptation of *A. fumigatus*. The deletion of the *rcfB* gene (see Fig. S10B in the supplemental material) led to a general slight delay in growth, which was independent of the oxygen partial pressure. However, the sporulation of the Δ*rcfB* mutant strain was delayed after 2 days of incubation under mild hypoxia (1% pO_2) compared to that of the wild-type strain (Fig. 8).

DISCUSSION

This study investigated the transcriptional response of *A. fumigatus* to hypoxia. Many similarities in the adaptation to hypoxia can be found when comparing our results with those from previous studies of *Aspergillus* species. As observed for *A. nidulans* and *A. oryzae* (18, 20), intracellular trafficking processes and cytoskeletal

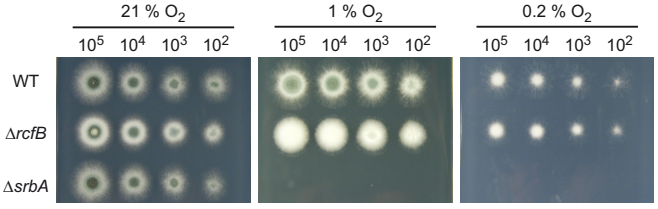

FIG 8 Growth of the *A. fumigatus* Δ*rcfB* strain under normoxic and hypoxic conditions. The wild-type and Δ*rcfB* and Δ*srbA* deletion strains were grown on AMM agar plates under normoxia or hypoxia with a partial pressure of either 1% pO_2 or 0.2% pO_2. Spores were serially diluted in H_2O, and 5 μl containing 10^5 to 10^2 spores was inoculated on the plates. Agar plates were incubated for 48 h at 37°C and 5% CO_2.

transcripts were downregulated under hypoxic conditions, most probably in order to reduce ATP consumption. In contrast, genes participating in the glyoxylate pathway were upregulated under hypoxic conditions, whereas the regulation of glycolytic genes was heterogenous (see Data Set S1 in the supplemental material). In this aspect, the hypoxic response of *A. fumigatus* resembles that of *A. oryzae* (18). The induction of the glyoxylate cycle may help to avoid NADH accumulation by bypassing two NADH-producing steps of the TCA cycle. The increased levels of transcripts contributing to amino acid transport are consistent with results from *A. nidulans* (18) and may point to increased production of specific amino acids under hypoxia.

In a previous study, we characterized the adaptation of *A. fumigatus* to hypoxia in a batch fermenter within a time window of 2 to 24 h (defined here as short-term response). Although the growth conditions were different (shorter incubation, batch fermentation, and excess of glucose), as described here, cell wall and sterol biosynthesis transcripts were upregulated (12). Similarly, with regard to respiration, complex IV-associated transcripts were increased in response to hypoxia.

Based on the obtained transcriptome data undertaken in this study, we tested our hypothesis regarding the impact of alternative respiration in *A. fumigatus* during growth under long-term hypoxic conditions. We aimed to elucidate the role of the single respiratory complexes in the adaptation process of *A. fumigatus* to hypoxia by using specific respiratory inhibitors. In addition, we analyzed the impact of alternative electron acceptors, such as nitrate and fumarate, on hypoxic growth of *A. fumigatus* in more detail by the generation of specific knockout strains.

Several microorganisms, including different bacterial and fungal species, make use of alternative electron acceptors, such as nitrate, when oxygen is limited (41–45). Indeed, our microarray experiment indicated that transcripts associated with nitrogen metabolism significantly increased in response to hypoxic growth conditions. The transcript level of the assimilatory nitrite reductase gene *niiA* was significantly induced, whereas the expression of

the nitrate reductase gene *niaD* was only slightly affected. Northern blot analysis revealed a slight increase in transcription levels of *niiA* and *niaD*. However, our previous proteome study analyzing the long-term response of *A. fumigatus* to hypoxia did not provide any evidence for NAD^+ regeneration via nitrate reduction (13). In line with this observation, the deletion of the assimilatory nitrate and nitrite reductases did not affect growth under hypoxic conditions. This suggests that in *A. fumigatus*, in contrast to *A. nidulans*, nitrate reduction does not significantly support growth under hypoxia (22, 23). In *F. oxysporum* and *Cylindrocarpon tonkinense*, membrane-bound, dissimilatory nitrate and nitrite reductases (dNaR and dNiR, respectively) were found to be part of a fungal denitrifying system, which is localized in the mitochondria, coupling with the electron transport chain to generate ATP under oxygen-limited conditions (42, 56, 57). Among them the fungal dNiR protein (*nirK*) of *F. oxysporum*, which is a copper-containing nitrite reductase, was found to be the eukaryotic ortholog of the bacterial counterpart. The C-terminal dNiR domain of *nirK* of *F. oxysporum* shares 76% identity with the respective amino acid sequence of the multicopper oxidase in *A. fumigatus* (58). This protein was also found in our microarray analyses to be induced upon oxygen limitation (Table 1). However, deletion mutants for this gene (AFUA_3G14950) were indistinguishable from the wild type irrespective of the O_2 levels (data not shown).

The increased expression of transcripts associated with nitrate/nitrite reduction may also be explained by a putative role of these enzymes in RNI detoxification. For example, a contribution of nitrite reductase to NO management in an oxygen-limited environment has been reported for bacteria like *E. coli* (59). Indeed, under low oxygen concentrations NO levels may increase, since the mitochondrial respiratory chain complex is capable of producing NO by reducing NO_2^- (14, 15, 46–49). This oxygen-independent process, which is activated under hypoxic or anoxic conditions, is catalyzed by the cytochrome *c* oxidase Cco (14, 15).

Commonly, flavohemoglobins detoxify harmful NO within the fungal cell (60, 61). In our microarray analyses, the flavohemoglobin gene *fhpA* was found to be upregulated by a factor of 17 upon exposure to hypoxia, which is consistent with results obtained from previous proteomic studies (12, 13). In the presence of nitrate, *fhpA* was induced over the entire time course of hypoxia, whereas *fhpA* was only upregulated within the first 3 h of hypoxia when using glutamine as the nitrogen source. This observation was further confirmed by fluorescence microscopy studies of an FhpA-eGFP fusion strain. Thus, we could demonstrate that the expression of *fhpA* is induced independently of the available nitrogen source under hypoxia. This favors the idea that elevated amounts of RNS are produced during hypoxia, although their origin is currently unknown.

FhpA utilizes O_2 and NAD(P)H to convert NO to NO_3^-. This oxygen dependence of NO detoxification supports the idea that alternative, reductive enzymes, such as the nitrite reductase NiiA, may take over the function of FhpA under hypoxia. Alternatively, the induction of NiiA may be explained by a spontaneous oxidation of NO to NO_2^- (62). However, there was only a moderate induction of *niiA* expression during hypoxia in the Northern blot analysis. In addition, the Δ*niiA* deletion mutant showed only sensitivity against NO_2^- at acidic pH, but not in the presence of the NO donor DETA-NO.

None of the deletion mutants was growth impaired in hypoxia. Thus, we conclude that the increased expression of FhpA and nitrate and nitrite reductases was caused by NO formation under hypoxia rather than by the hypoxic conditions itself.

Overall, in *A. fumigatus*, nitrate reduction does not seem to provide a mechanism to reload the pool of $NAD(P)^+$ or FAD^+ when O_2 becomes limiting. Alternatively, the reduction of fumarate to succinate is linked with the regeneration of NAD^+ and may function as an electron sink, as described for *Mycobacterium tuberculosis* (63). Also, the fungal species *Aspergillus niger*, *A. oryzae*, and *S. cerevisae* produce elevated amounts of succinate under oxygen-limiting conditions (18, 52, 64). Gene expression of the cytosolic fumarate reductase *frdA* was significantly induced in *A. fumigatus* during hypoxia, and succinate was detectable in the supernatant of hypoxic batch cultures.

However, transcript levels of the mitochondrial fumarate reductase gene *osmA* remained constant and thus were not affected by oxygen availability. These findings are consistent with the reported regulation of the fumarate reductase genes *frd1* and *osm1* in *S. cerevisae* during anaerobiosis (52). Contrary to *S. cerevisae*, in *A. fumigatus* deletion of fumarate reductases in single or double knockout strains had no effect on the growth phenotype under hypoxia (51). Besides NAD^+ regeneration, other functions have been suggested for fumarate reductases, in particular redox balancing during anaerobiosis and the reoxidation of flavin cofactors (52, 65, 66). In line with this assumption, the *A. fumigatus* Δ*frdA*, Δ*osmA*, and Δ*frdA* Δ*osmA* fumarate reductase deletion strains were more susceptible to the reducing agent TCEP, which affects the intracellular redox homeostasis. In summary, the *A. fumigatus* fumarate reductase gene *frdA* may be highly upregulated during hypoxia to maintain redox homeostasis. Hence, our study supports the hypothesis that the expression of fumarate reductase is upregulated during hypoxia to reoxidize flavin cofactors and thus to keep flavoenzymes in their oxidized state.

Our data and previous studies on *A. fumigatus* and other fungi indicated an association of functional mitochondria with the ability to adapt to low-oxygen environments (11, 17, 67–70). The upregulation of several respiratory genes during long-term exposure to hypoxia is also consistent with the increased production of components of the electron transport chain and oxidative phosphorylation on the proteome level (12, 13). Besides the classical electron transport chain via complexes I to IV, fungi and plants possess alternative routes: the alternative NADH:ubiquinone oxidoreductase (a bypass of complex I) and the alternative oxidase AOX, which bypasses complexes III and IV (53, 54). For this study we aimed at investigating the role of each respiratory complex in the adaptation process of *A. fumigatus* toward hypoxia.

Complex I transfers electrons from NADH to ubiquinone and thus is essential for the regeneration of NAD^+. Its specific inhibition with rotenone resulted in only a slight reduction of growth of *A. fumigatus* under hypoxia. Interestingly, it was shown that rotenone only partially inhibits the oxidation of NADH in *A. fumigatus* (71). Hence, the low inhibitory effect of rotenone might be due to a compensatory reaction of alternative NADH dehydrogenases. These can be specifically inhibited by flavone (71). In the presence of flavone, growth of *A. fumigatus* was reduced independently of the level of oxygen. Even the combination of flavone and rotenone had no significant effect on the hypoxic growth of *A. fumigatus*, indicating that complex I and the alternative NADH:ubiquinone oxidoreductase are not absolutely essential during hypoxic growth. This suggests that bypass routes exist under oxygen-lim-

iting conditions and electrons may enter the quinone pool independently of complex I.

Succinate dehydrogenase (complex II) oxidizes succinate to fumarate and transfers the electrons to ubiquinone. Disodium malonate is a competitive inhibitor of complex II (54). However, the inhibitory effect of disodium malonate on the growth of *A. fumigatus* was independent of the oxygen availability, indicating a minor role of complex II in the adaptation process of the fungi toward hypoxia.

Electrons of the ubiquinone pool can be either transferred to oxygen via cytochrome *c* by complexes III and IV or by the alternative oxidase (53, 54). We could demonstrate that the alternative oxidase, AOX, is not essential for hypoxic growth since inhibition of AOX was independent of the oxygen availability. In agreement with our data, hypoxic growth of the *A. fumigatus* Δ*aox* strain was like that of the wild type (11). Interestingly, under normoxic conditions a strain deleted for *srbA* was more susceptible to the alternative oxidase inhibitor SHAM. Although transcript levels of *aox* were increased in the Δ*srbA* mutant, no altered gene expression could be observed for cytochrome *c*. These data indicate that in the Δ*srbA* mutant, electron transport proceeds via complexes III and IV but is also partially dependent on AOX, as illustrated by the upregulation of the corresponding *aox* gene in the mutant. Recently, it was demonstrated that besides electron transport, the alternative oxidase is also involved in the oxidative stress response and macrophage killing of *A. fumigatus* (11). Remarkably, inhibition of complex III by antimycin A provoked a strong growth defect of *A. fumigatus* during hypoxia in a dose-dependent manner of the inhibitor, which was not observed under normoxic conditions. Furthermore, in the presence of the complex IV inhibitor sodium azide, growth of *A. fumigatus* was significantly reduced under hypoxic compared to normoxic conditions. Additionally, we could demonstrate that the transcripts of the cytochrome *c* oxidase subunit *coxVb* and the *rcf2*-like gene *rcfB* increased during hypoxia. These findings are consistent with the increased abundance of components of respiratory complexes III and IV in our proteome study of the long-term response of *A. fumigatus* to hypoxia (13). In this context, it is interesting to note that in *S. cerevisiae coxVb* is the more active isoform during hypoxia, whereas *coxVa* represents the dominating aerobic isoform (72). The proteins Rcf1 and Rcf2 are members of the hypoxia-induced gene 1 (Hig1) protein family and are involved in the assembly of the cytochrome *c* oxidase supercomplex in yeast (37). Although the *A. fumigatus* Δ*rcfB* deletion strain was still able to grow, reduced formation of conidia was observed during mild hypoxia (1% O_2). Remarkably Rcf1 is required for hypoxic growth in yeast (55). However, transcripts of the corresponding *rcf1* homologue in *A. fumigatus* were not found to be differentially regulated in our microarray data.

Overall, in *A. fumigatus* a functional electron transport chain obviously plays an essential role for hypoxic growth. This particularly applies to respiratory complexes III and IV, which might be involved in sensing and adapting to hypoxia by posttranslational protein modifications, e.g., nitrotyrosination (16, 17).

In conclusion, this study analyzed the impact of aerobic respiration and reductive pathways on hypoxic growth of *A. fumigatus*. Characterization of the *A. fumigatus* Δ*niiA*, Δ*niaD*, Δ*frdA*, Δ*osmA* and Δ*frdA* Δ*osmA* deletion strains revealed that neither nitrate nor fumarate was used as an alternative electron acceptor under oxygen-limiting conditions. In accordance with this finding, we were able to demonstrate that a functional electron transport chain, especially complexes III and IV, is essential for the adaptation of *A. fumigatus* toward hypoxic growth conditions.

ACKNOWLEDGMENTS

This work was supported by funding from the German-Israeli Foundation for Scientific Research and Development (GIF no. 996-47.12/2008), the ERA-Net Pathogenomics project OXYstress, and the International Leibniz Research School (ILRS) for Microbial and Biomolecular Interactions as part of the DFG-funded Excellence Graduate School Jena School for Microbial Communication (JSMC).

REFERENCES

1. **Tekaia F, Latge JP.** 2005. *Aspergillus fumigatus*: saprophyte or pathogen? Curr. Opin. Microbiol. **8:**385–392. http://dx.doi.org/10.1016/j.mib.2005.06.017.
2. **Rhodes JC.** 2006. *Aspergillus fumigatus*: growth and virulence. Med. Mycol. **44**(Suppl 1)**:**S77–S81. http://dx.doi.org/10.1080/13693780600779419.
3. **Latge JP.** 2001. The pathobiology of *Aspergillus fumigatus*. Trends Microbiol. **9:**382–389. http://dx.doi.org/10.1016/S0966-842X(01)02104-7.
4. **Brakhage AA, Bruns S, Thywissen A, Zipfel PF, Behnsen J.** 2010. Interaction of phagocytes with filamentous fungi. Curr. Opin. Microbiol. **13:**409–415. http://dx.doi.org/10.1016/j.mib.2010.04.009.
5. **Brakhage AA.** 2005. Systemic fungal infections caused by *Aspergillus* species: epidemiology, infection process and virulence determinants. Curr. Drug Targets **6:**875–886. http://dx.doi.org/10.2174/138945005774912717.
6. **Jain M, Sznajder JI.** 2005. Effects of hypoxia on the alveolar epithelium. Proc. Am. Thorac. Soc. **2:**202–205. http://dx.doi.org/10.1513/pats.200501-006AC.
7. **Lewis JS, Lee JA, Underwood JC, Harris AL, Lewis CE.** 1999. Macrophage responses to hypoxia: relevance to disease mechanisms. J. Leukoc. Biol. **66:**889–900.
8. **Grahl N, Shepardson KM, Chung D, Cramer RA.** 2012. Hypoxia and fungal pathogenesis: to air or not to air? Eukaryot. Cell **11:**560–570. http://dx.doi.org/10.1128/EC.00031-12.
9. **Willger SD, Puttikamonkul S, Kim KH, Burritt JB, Grahl N, Metzler LJ, Barbuch R, Bard M, Lawrence CB, Cramer RA, Jr.** 2008. A sterol-regulatory element binding protein is required for cell polarity, hypoxia adaptation, azole drug resistance, and virulence in *Aspergillus fumigatus*. PLoS Pathog. **4:**e1000200. http://dx.doi.org/10.1371/journal.ppat.1000200.
10. **Hall LA, Denning DW.** 1994. Oxygen requirements of *Aspergillus* species. J. Med. Microbiol. **41:**311–315. http://dx.doi.org/10.1099/00222615-41-5-311.
11. **Grahl N, Dinamarco TM, Willger SD, Goldman GH, Cramer RA.** 2012. *Aspergillus fumigatus* mitochondrial electron transport chain mediates oxidative stress homeostasis, hypoxia responses and fungal pathogenesis. Mol. Microbiol. **84:**383–399. http://dx.doi.org/10.1111/j.1365-2958.2012.08034.x.
12. **Barker BM, Kroll K, Vodisch M, Mazurie A, Kniemeyer O, Cramer RA.** 2012. Transcriptomic and proteomic analyses of the *Aspergillus fumigatus* hypoxia response using an oxygen-controlled fermenter. BMC Genomics **13:**62. http://dx.doi.org/10.1186/1471-2164-13-62.
13. **Vödisch M, Scherlach K, Winkler R, Hertweck C, Braun HP, Roth M, Haas H, Werner ER, Brakhage AA, Kniemeyer O.** 2011. Analysis of the *Aspergillus fumigatus* proteome reveals metabolic changes and the activation of the pseurotin A biosynthesis gene cluster in response to hypoxia. J. Proteome Res. **10:**2508–2524. http://dx.doi.org/10.1021/pr1012812.
14. **Castello PR, David PS, McClure T, Crook Z, Poyton RO.** 2006. Mitochondrial cytochrome oxidase produces nitric oxide under hypoxic conditions: implications for oxygen sensing and hypoxic signaling in eukaryotes. Cell Metab. **3:**277–287. http://dx.doi.org/10.1016/j.cmet.2006.02.011.
15. **Castello PR, Woo DK, Ball K, Wojcik J, Liu L, Poyton RO.** 2008. Oxygen-regulated isoforms of cytochrome c oxidase have differential effects on its nitric oxide production and on hypoxic signaling. Proc. Natl. Acad. Sci. U. S. A. **105:**8203–8208. http://dx.doi.org/10.1073/pnas.0709461105.
16. **Poyton RO, Castello PR, Ball KA, Woo DK, Pan N.** 2009. Mitochondria and hypoxic signaling: a new view. Ann. N. Y. Acad. Sci. **1177:**48–56. http://dx.doi.org/10.1111/j.1749-6632.2009.05046.x.
17. **Poyton RO, Ball KA, Castello PR.** 2009. Mitochondrial generation of free

radicals and hypoxic signaling. Trends Endocrinol. Metab. **20:**332–340. http://dx.doi.org/10.1016/j.tem.2009.04.001.

18. **Terabayashi Y, Shimizu M, Kitazume T, Masuo S, Fujii T, Takaya N.** 2012. Conserved and specific responses to hypoxia in *Aspergillus oryzae* and *Aspergillus nidulans* determined by comparative transcriptomics. Appl. Microbiol. Biotechnol. **93:**305–317. http://dx.doi.org/10.1007/s00253-011-3767-4.
19. **Grahl N, Puttikamonkul S, Macdonald JM, Gamcsik MP, Ngo LY, Hohl TM, Cramer RA.** 2011. In vivo hypoxia and a fungal alcohol dehydrogenase influence the pathogenesis of invasive pulmonary aspergillosis. PLoS Pathog. **7:**e1002145. http://dx.doi.org/10.1371/journal.ppat.1002145.
20. **Masuo S, Terabayashi Y, Shimizu M, Fujii T, Kitazume T, Takaya N.** 2010. Global gene expression analysis of *Aspergillus nidulans* reveals metabolic shift and transcription suppression under hypoxia. Mol. Genet. Genomics **284:**415–424. http://dx.doi.org/10.1007/s00438-010-0576-x.
21. **Shimizu M, Fujii T, Masuo S, Fujita K, Takaya N.** 2009. Proteomic analysis of *Aspergillus nidulans* cultured under hypoxic conditions. Proteomics **9:**7–19. http://dx.doi.org/10.1002/pmic.200701163.
22. **Takasaki K, Shoun H, Yamaguchi M, Takeo K, Nakamura A, Hoshino T, Takaya N.** 2004. Fungal ammonia fermentation, a novel metabolic mechanism that couples the dissimilatory and assimilatory pathways of both nitrate and ethanol. Role of acetyl CoA synthetase in anaerobic ATP synthesis. J. Biol. Chem. **279:**12414–12420. http://dx.doi.org/10.1074/jbc.M313761200.
23. **Zhou Z, Takaya N, Nakamura A, Yamaguchi M, Takeo K, Shoun H.** 2002. Ammonia fermentation, a novel anoxic metabolism of nitrate by fungi. J. Biol. Chem. **277:**1892–1896. http://dx.doi.org/10.1074/jbc.M109096200.
24. **Brakhage AA, Van den Brulle J.** 1995. Use of reporter genes to identify recessive *trans*-acting mutations specifically involved in the regulation of *Aspergillus nidulans* penicillin biosynthesis genes. J. Bacteriol. **177:**2781–2788.
25. **Gehrke A, Heinekamp T, Jacobsen ID, Brakhage AA.** 2010. Heptahelical receptors GprC and GprD of *Aspergillus fumigatus* are essential regulators of colony growth, hyphal morphogenesis, and virulence. Appl. Environ. Microbiol. **76:**3989–3998. http://dx.doi.org/10.1128/AEM.00052-10.
26. **Nierman WC, Pain A, Anderson MJ, Wortman JR, Kim HS, Arroyo J, Berriman M, Abe K, Archer DB, Bermejo C, Bennett J, Bowyer P, Chen D, Collins M, Coulsen R, Davies R, Dyer PS, Farman M, Fedorova N, Fedorova N, Feldblyum TV, Fischer R, Fosker N, Fraser A, Garcia JL, Garcia MJ, Goble A, Goldman GH, Gomi K, Griffith-Jones S, Gwilliam R, Haas B, Haas H, Harris D, Horiuchi H, Huang J, Humphray S, Jimenez J, Keller N, Khouri H, Kitamoto K, Kobayashi T, Konzack S, Kulkarni R, Kumagai T, Lafon A, Latge JP, Li W, Lord A, Lu C, Majoros WH, May GS, Miller BL, Mohamoud Y, Molina M, Monod M, Mouyna I, Mulligan S, Murphy L, O'Neil S, Paulsen I, Penalva MA, Pertea M, Price C, Pritchard BL, Quail MA, Rabbinowitsch E, Rawlins N, Rajandream MA, Reichard U, Renauld H, Robson GD, Rodriguez de Cordoba S, Rodriguez-Pena JM, Ronning CM, Rutter S, Salzberg SL, Sanchez M, Sanchez-Ferrero JC, Saunders D, Seeger K, Squares R, Squares S, Takeuchi M, Tekaia F, Turner G, Vazquez de Aldana CR, Weidman J, White O, Woodward J, Yu JH, Fraser C, Galagan JE, Asai K, Machida M, Hall N, Barrell B, Denning DW.** 2005. Genomic sequence of the pathogenic and allergenic filamentous fungus *Aspergillus fumigatus*. Nature **438:**1151–1156. http://dx.doi.org/10.1038/nature04332.
27. **Smyth GK.** 2005. Limma: linear models for microarray data, p 97–420. *In* Gentleman R, Carey V, Huber W, Irizarry R, Dudoit S (ed), Bioinformatics and computational biology solutions using R and Bioconductor. Springer, New York, NY.
28. **Gentleman RC, Carey VJ, Bates DM, Bolstad B, Dettling M, Dudoit S, Ellis B, Gautier L, Ge Y, Gentry J, Hornik K, Hothorn T, Huber W, Iacus S, Irizarry R, Leisch F, Li C, Maechler M, Rossini AJ, Sawitzki G, Smith C, Smyth G, Tierney L, Yang JY, Zhang J.** 2004. Bioconductor: open software development for computational biology and bioinformatics. Genome Biol. **5:**R80. http://dx.doi.org/10.1186/gb-2004-5-10-r80.
29. **da Silva Ferreira ME, Kress MR, Savoldi M, Goldman MH, Hartl A, Heinekamp T, Brakhage AA, Goldman GH.** 2006. The akuB(KU80) mutant deficient for nonhomologous end joining is a powerful tool for analyzing pathogenicity in *Aspergillus fumigatus*. Eukaryot. Cell **5:**207–211. http://dx.doi.org/10.1128/EC.5.1.207-211.2006.
30. **Weidner G, d'Enfert C, Koch A, Mol PC, Brakhage AA.** 1998. Development of a homologous transformation system for the human pathogenic fungus *Aspergillus fumigatus* based on the pyrG gene encoding orotidine 5′-monophosphate decarboxylase. Curr. Genet. **33:**378–385. http://dx.doi.org/10.1007/s002940050350.
31. **Liebmann B, Muller M, Braun A, Brakhage AA.** 2004. The cyclic AMP-dependent protein kinase a network regulates development and virulence in *Aspergillus fumigatus*. Infect. Immun. **72:**5193–5203. http://dx.doi.org/10.1128/IAI.72.9.5193-5203.2004.
32. **Szewczyk E, Krappmann S.** 2010. Conserved regulators of mating are essential for *Aspergillus fumigatus* cleistothecium formation. Eukaryot. Cell **9:**774–783. http://dx.doi.org/10.1128/EC.00375-09.
33. **Aichinger C, Hansson K, Eichhorn H, Lessing F, Mannhaupt G, Mewes W, Kahmann R.** 2003. Identification of plant-regulated genes in *Ustilago maydis* by enhancer-trapping mutagenesis. Mol. Genet. Genomics **270:**303–314. http://dx.doi.org/10.1007/s00438-003-0926-z.
34. **Collopy PD, Colot HV, Park G, Ringelberg C, Crew CM, Borkovich KA, Dunlap JC.** 2010. High-throughput construction of gene deletion cassettes for generation of *Neurospora crassa* knockout strains. Methods Mol. Biol. **638:**33–40. http://dx.doi.org/10.1007/978-1-60761-611-5_3.
35. **Levdansky E, Romano J, Shadkchan Y, Sharon H, Verstrepen KJ, Fink GR, Osherov N.** 2007. Coding tandem repeats generate diversity in *Aspergillus fumigatus* genes. Eukaryot. Cell **6:**1380–1391. http://dx.doi.org/10.1128/EC.00229-06.
36. **Jacobsen ID, Grosse K, Slesiona S, Hube B, Berndt A, Brock M.** 2010. Embryonated eggs as an alternative infection model to investigate *Aspergillus fumigatus* virulence. Infect. Immun. **78:**2995–3006. http://dx.doi.org/10.1128/IAI.00268-10.
37. **Strogolova V, Furness A, Robb-McGrath M, Garlich J, Stuart RA.** 2012. Rcf1 and Rcf2, members of the hypoxia-induced gene 1 protein family, are critical components of the mitochondrial cytochrome bc1-cytochrome c oxidase supercomplex. Mol. Cell. Biol. **32:**1363–1373. http://dx.doi.org/10.1128/MCB.06369-11.
38. **Vukotic M, Oeljeklaus S, Wiese S, Vögtle FN, Meisinger C, Meyer HE, Zieseniss A, Katschinski DM, Jans DC, Jakobs S, Warscheid B, Rehling P, Deckers M.** 2012. Rcf1 mediates cytochrome oxidase assembly and respirasome formation, revealing heterogeneity of the enzyme complex. Cell Metab. **15:**336–347. http://dx.doi.org/10.1016/j.cmet.2012.01.016.
39. **Zhou S, Fushinobu S, Nakanishi Y, Kim SW, Wakagi T, Shoun H.** 2009. Cloning and characterization of two flavohemoglobins from *Aspergillus oryzae*. Biochem. Biophys. Res. Commun. **381:**7–11. http://dx.doi.org/10.1016/j.bbrc.2009.01.112.
40. **Schinko T, Berger H, Lee W, Gallmetzer A, Pirker K, Pachlinger R, Buchner I, Reichenauer T, Guldener U, Strauss J.** 2010. Transcriptome analysis of nitrate assimilation in *Aspergillus nidulans* reveals connections to nitric oxide metabolism. Mol. Microbiol. **78:**720–738. http://dx.doi.org/10.1111/j.1365-2958.2010.07363.x.
41. **Shoun H, Kim DH, Uchiyama H, Sugiyama J.** 1992. Denitrification by fungi. FEMS Microbiol. Lett. **73:**277–281.
42. **Kobayashi M, Matsuo Y, Takimoto A, Suzuki S, Maruo F, Shoun H.** 1996. Denitrification, a novel type of respiratory metabolism in fungal mitochondrion. J. Biol. Chem. **271:**16263–16267. http://dx.doi.org/10.1074/jbc.271.27.16263.
43. **Nakano MM, Zuber P.** 1998. Anaerobic growth of a "strict aerobe" (*Bacillus subtilis*). Annu. Rev. Microbiol. **52:**165–190. http://dx.doi.org/10.1146/annurev.micro.52.1.165.
44. **Unden G, Bongaerts J.** 1997. Alternative respiratory pathways of *Escherichia coli*: energetics and transcriptional regulation in response to electron acceptors. Biochim. Biophys. Acta **1320:**217–234. http://dx.doi.org/10.1016/S0005-2728(97)00034-0.
45. **Fujii T, Takaya N.** 2008. Denitrification by the fungus *Fusarium oxysporum* involves NADH-nitrate reductase. Biosci. Biotechnol. Biochem. **72:**412–420. http://dx.doi.org/10.1271/bbb.70538.
46. **Tischner R, Planchet E, Kaiser WM.** 2004. Mitochondrial electron transport as a source for nitric oxide in the unicellular green alga *Chlorella sorokiniana*. FEBS Lett. **576:**151–155. http://dx.doi.org/10.1016/j.febslet.2004.09.004.
47. **Planchet E, Jagadis Gupta K, Sonoda M, Kaiser WM.** 2005. Nitric oxide emission from tobacco leaves and cell suspensions: rate limiting factors and evidence for the involvement of mitochondrial electron transport. Plant J. **41:**732–743. http://dx.doi.org/10.1111/j.1365-313X.2005.02335.x.
48. **Lacza Z, Kozlov AV, Pankotai E, Csordas A, Wolf G, Redl H, Kollai M, Szabo C, Busija DW, Horn TF.** 2006. Mitochondria produce reactive nitrogen species via an arginine-independent pathway. Free Radic. Res. **40:**369–378. http://dx.doi.org/10.1080/10715760500539139.

49. **Igamberdiev AU, Hill RD.** 2009. Plant mitochondrial function during anaerobiosis. Ann. Bot. **103:**259–268. http://dx.doi.org/10.1093/aob/mcn100.
50. **Stamler JS, Singel DJ, Loscalzo J.** 1992. Biochemistry of nitric oxide and its redox-activated forms. Science **258:**1898–1902. http://dx.doi.org/10.1126/science.1281928.
51. **Arikawa Y, Enomoto K, Muratsubaki H, Okazaki M.** 1998. Soluble fumarate reductase isoenzymes from *Saccharomyces cerevisiae* are required for anaerobic growth. FEMS Microbiol. Lett. **165:**111–116. http://dx.doi.org/10.1111/j.1574-6968.1998.tb13134.x.
52. **Camarasa C, Faucet V, Dequin S.** 2007. Role in anaerobiosis of the isoenzymes for *Saccharomyces cerevisiae* fumarate reductase encoded by OSM1 and FRDS1. Yeast **24:**391–401. http://dx.doi.org/10.1002/yea.1467.
53. **Joseph-Horne T, Hollomon DW, Wood PM.** 2001. Fungal respiration: a fusion of standard and alternative components. Biochim. Biophys. Acta **1504:**179–195. http://dx.doi.org/10.1016/S0005-2728(00)00251-6.
54. **Martins VdP, Dinamarco TM, Curti C, Uyemura SA.** 2011. Classical and alternative components of the mitochondrial respiratory chain in pathogenic fungi as potential therapeutic targets. J. Bioenerg. Biomembr. **43:**81–88. http://dx.doi.org/10.1007/s10863-011-9331-1.
55. **Vukotic M, Oeljeklaus S, Wiese S, Vogtle FN, Meisinger C, Meyer HE, Zieseniss A, Katschinski DM, Jans DC, Jakobs S, Warscheid B, Rehling P, Deckers M.** 2012. Rcf1 mediates cytochrome oxidase assembly and respirasome formation, revealing heterogeneity of the enzyme complex. Cell Metab. **15:**336–347. http://dx.doi.org/10.1016/j.cmet.2012.01.016.
56. **Shoun H, Tanimoto T.** 1991. Denitrification by the fungus *Fusarium oxysporum* and involvement of cytochrome P-450 in the respiratory nitrite reduction. J. Biol. Chem. **266:**11078–11082.
57. **Takaya N, Kuwazaki S, Adachi Y, Suzuki S, Kikuchi T, Nakamura H, Shiro Y, Shoun H.** 2003. Hybrid respiration in the denitrifying mitochondria of *Fusarium oxysporum*. J. Biochem. **133:**461–465. http://dx.doi.org/10.1093/jb/mvg060.
58. **Kim SW, Fushinobu S, Zhou S, Wakagi T, Shoun H.** 2009. Eukaryotic nirK genes encoding copper-containing nitrite reductase: originating from the protomitochondrion? Appl. Environ. Microbiol. **75:**2652–2658. http://dx.doi.org/10.1128/AEM.02536-08.
59. **Poock SR, Leach ER, Moir JW, Cole JA, Richardson DJ.** 2002. Respiratory detoxification of nitric oxide by the cytochrome c nitrite reductase of *Escherichia coli*. J. Biol. Chem. **277:**23664–23669. http://dx.doi.org/10.1074/jbc.M200731200.
60. **Gardner PR.** 2005. Nitric oxide dioxygenase function and mechanism of flavohemoglobin, hemoglobin, myoglobin and their associated reductases. J. Inorg. Biochem. **99:**247–266. http://dx.doi.org/10.1016/j.jinorgbio.2004.10.003.
61. **Forrester MT, Foster MW.** 2012. Protection from nitrosative stress: a central role for microbial flavohemoglobin. Free Radic. Biol. Med. **52:**1620–1633. http://dx.doi.org/10.1016/j.freeradbiomed.2012.01.028.
62. **Yamasaki H.** 2000. Nitrite-dependent nitric oxide production pathway: implications for involvement of active nitrogen species in photoinhibition in vivo. Philos. Trans. R. Soc. Lond. B Biol. Sci. **355:**1477–1488. http://dx.doi.org/10.1098/rstb.2000.0708.
63. **Watanabe S, Zimmermann M, Goodwin MB, Sauer U, Barry CE, III, Boshoff HI.** 2011. Fumarate reductase activity maintains an energized membrane in anaerobic *Mycobacterium tuberculosis*. PLoS Pathog. **7:**e1002287. http://dx.doi.org/10.1371/journal.ppat.1002287.
64. **Diano A, Peeters J, Dynesen J, Nielsen J.** 2009. Physiology of *Aspergillus niger* in oxygen-limited continuous cultures: influence of aeration, carbon source concentration and dilution rate. Biotechnol. Bioeng. **103:**956–965. http://dx.doi.org/10.1002/bit.22329.
65. **Enomoto K, Arikawa Y, Muratsubaki H.** 2002. Physiological role of soluble fumarate reductase in redox balancing during anaerobiosis in *Saccharomyces cerevisiae*. FEMS Microbiol. Lett. **215:**103–108. http://dx.doi.org/10.1111/j.1574-6968.2002.tb11377.x.
66. **Sedzielewska KA, Boer E, Bellebna C, Wartmann T, Bode R, Melzer M, Baronian K, Kunze G.** 2012. Role of the AFRD1-encoded fumarate reductase in hypoxia and osmotolerance in *Arxula adeninivorans*. FEMS Yeast Res. **12:**924–937. http://dx.doi.org/10.1111/j.1567-1364.2012.00842.x.
67. **Ingavale SS, Chang YC, Lee H, McClelland CM, Leong ML, Kwon-Chung KJ.** 2008. Importance of mitochondria in survival of *Cryptococcus neoformans* under low oxygen conditions and tolerance to cobalt chloride. PLoS Pathog. **4:**e1000155. http://dx.doi.org/10.1371/journal.ppat.1000155.
68. **Guzy RD, Mack MM, Schumacker PT.** 2007. Mitochondrial complex III is required for hypoxia-induced ROS production and gene transcription in yeast. Antioxid. Redox Signal. **9:**1317–1328. http://dx.doi.org/10.1089/ars.2007.1708.
69. **David PS, Poyton RO.** 2005. Effects of a transition from normoxia to anoxia on yeast cytochrome c oxidase and the mitochondrial respiratory chain: implications for hypoxic gene induction. Biochim. Biophys. Acta **1709:**169–180. http://dx.doi.org/10.1016/j.bbabio.2005.07.002.
70. **Kwast KE, Burke PV, Staahl BT, Poyton RO.** 1999. Oxygen sensing in yeast: evidence for the involvement of the respiratory chain in regulating the transcription of a subset of hypoxic genes. Proc. Natl. Acad. Sci. U. S. A. **96:**5446–5451. http://dx.doi.org/10.1073/pnas.96.10.5446.
71. **Tudella VG, Curti C, Soriani FM, Santos AC, Uyemura SA.** 2004. In situ evidence of an alternative oxidase and an uncoupling protein in the respiratory chain of *Aspergillus fumigatus*. Int. J. Biochem. Cell Biol. **36:**162–172. http://dx.doi.org/10.1016/S1357-2725(03)00194-8.
72. **Burke PV, Poyton RO.** 1998. Structure/function of oxygen-regulated isoforms in cytochrome c oxidase. J. Exp. Biol. **201:**1163–1175.